Design and Testing of an Origami-based Deployable Telescope System

Philip Klocke*, Trevor Carter*, Quinn Earnest*, Fisk Lundgreen*, Brooklyn Olson*, Jake Sutton*, Zhongyuan Wang*, Davis Wing*, Colin Peter†, Guangjun Gao‡, Nathan Usevitch‡, Spencer Magleby‡ and Larry Howell‡,

Introduction

Space-based optical systems are indispensable for observing and understanding both Earth and the broader universe [1, 2]. Light Detection and Ranging (LiDAR) systems in particular provide data on phenomena such as atmospheric dynamics, surface topography, ice sheet elevation, vegetation coverage, and ocean circulation [3, 4, 5, 6]. These measurements inform critical climate models, environmental monitoring, and disaster response planning. However, as LiDAR payloads grow increasingly sophisticated, they require larger optical apertures to achieve improved resolution and signal-to-noise performance. The challenge lies in fitting these large optical systems within the strict volume constraints of modern satellite launch vehicles, which has motivated the exploration of deployable, precision optical structures [7].

Origami-inspired engineering offers an elegant solution to the competing needs of compact stowage and large deployed surface area [8, 9]. Origami patterns can be folded into highly compact configurations and then deployed into functional, rigid structures with predictable kinematics [10]. Furthermore, origami folding principles can be applied to rigid materials, such as metals or ceramics by implementing thickness accommodation techniques [11, 12, 13]. Panel deformation is also avoided by using compliant surrogate hinges [14].

The origami “flasher” pattern (see Figure 1) is of particular interest for space applications requiring radial symmetry. The flasher pattern transforms a circular sheet into a compact spiral through a series of concentric and radial folds. From an engineering perspective, this geometry provides multiple advantages: it maintains circular symmetry desirable for optical systems, evenly distributes mechanical strain during folding, and enables predictable deployment dynamics about a central axis [15]. A circular optical array based on a flasher fold can therefore deploy uniformly and preserve optical alignment, while minimizing the required packaging volume. This rotationally symmetric deployment also simplifies actuator design and load distribution [16].

This work investigates the integration of flasher-inspired origami mechanisms with deployable LiDAR optical systems. The objective is to design a compact and thin structure, capable of achieving large-aperture deployment with optical-level alignment and repeatability. Figure 1 shows a conceptual rendering of the system. This enables LiDAR instruments to maintain optical performance while reducing stowed volume and lowering launch mass, benefiting a wide range of space-based optical applications and enabling more efficient and adaptive communication systems.

Methods

System Overview

An origami flasher pattern was selected as the basis for this work. Flashers represent a large family of origami patterns that are defined by a few parameters. “m” is the number of sides of the regular, central polygon (also the number of gores); “h” is the height order; “r” is the ring order; and “dr” is defined as “the

* Brigham Young University, Provo, UT, pklocke@byu.edu
† MMA Space, Broomfield, CO
‡ NASA Goddard Space Flight Center, Greenbelt, MD

desired separation between two nearest-neighbor vertices at the same radial position and the same z-coordinate, normalized to the diameter of the circumcircle of the central polygon" [16]. An initial explorative study was conducted to consider the ideal crease pattern that balanced deployed area, usable optical area, maximum panel size, and stowability, among other metrics. The selected flasher creases pattern had parameters m = 5, *h* = 2, *r* = 1, and *dr* = 0.1.

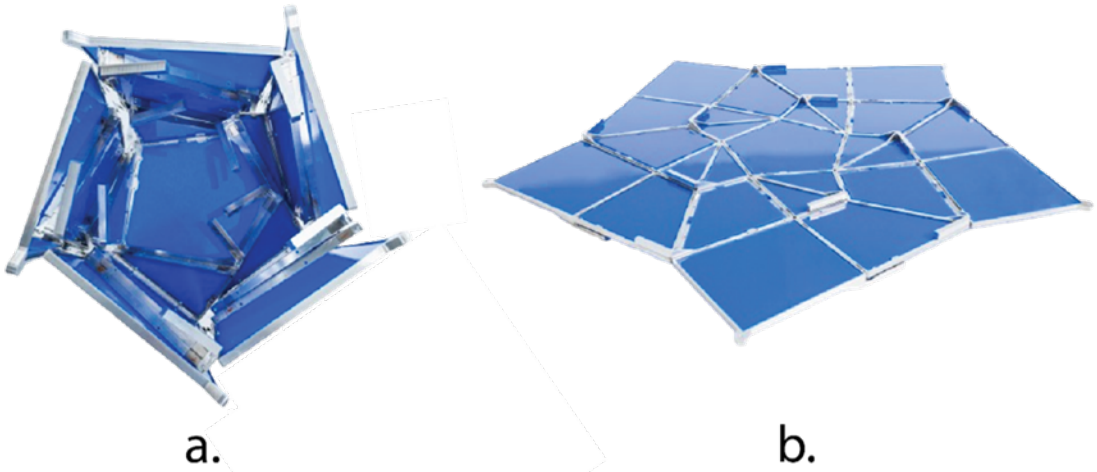

Figure 1. Image of the Telescope Mechanical System in the (a) Stowed State and (b) Deployed State

The system consists of the following elements: (1) Rigid aluminum frames that define each panel of the flasher, (2) kinematic couplings that ensure repeatable deployment, (3) compliant hinges that store elastic energy and help the array deploy, (4) deployable booms, (5) optical interfaces, and (6) an adjustment system within each frame for optical calibration.

Rigid aluminum frames were used to provide an appropriate housing for precision elements, optical components, and deployment mechanisms (see Figure 2(a-b)). The hinge shift technique was used to accommodate the thickness of the frames [13]. This technique shifts the axis of rotation between adjacent panels to either the upper or lower panel surfaces.

Kinematic couplings were strategically placed along each hinge in a petal (see Figure 2(a-b)). By connecting only those panels in each petal, the position of each panel throughout the telescope was repeatably defined without over-constraint.

Each kinematic coupling was uniquely designed to fit within the constrained space between adjacent panels. Each coupling was based on the modified kinematic coupling presented by Roubicek et al. and shown in Figure 3 [7]. Additional modified kinematic couplings were also proposed and tested for this telescope, which introduced extension arms to improve both its stability and repeatability (see Figure 4). These were placed at locations where sufficient volume existed in the stowed state so as to avoid interference during deployment.

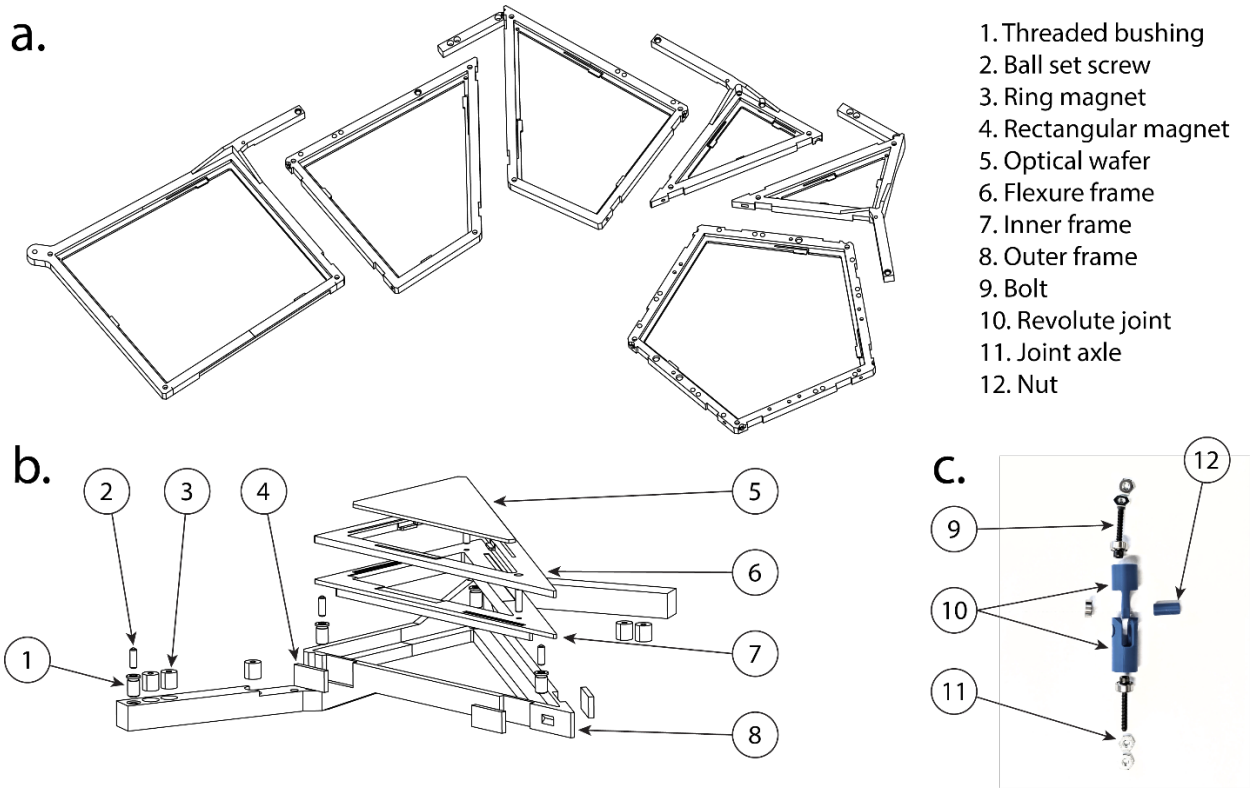

Figure 2. (a) Diagram of the 5 panels, constituting a "petal", and inner pentagon of the flasher telescope system. (b) Exploded view of a single panel, including the system that allows for adjustment within the frame. (c) Exploded image of the joints connecting the origami-based telescope to the deployment booms.

The ball and groove contacts of each coupling ensured that each degree of freedom was constrained in a repeatable manner in the deployed state. Additional design exploration and test results for these couplings are anticipated in a future publication. Magnets were used to provide a clamping force across each coupling in the deployed state, ensuring coupling contact was maintained. Test data for magnetic hinges has been previously published [17].

Compliant hinges were used to connect panels between petals. These hinges were based on a compacted Lamina Emergent Torsional (LET) joint [18] presented by Gardner et al. [19] (see Figure 4). The low stiffness of compact LET joints ensured a smooth deployment without interfering with the precision elements used to constraint the system in its deployed state. Furthermore, the strain energy stored by hinge deformation during stowage, in combination with the deployment booms, provided the required torques to deploy the system.

Deployment booms developed, tested, and proven by MMA Space [20], were used to take the flasher from the stowed state to deployed state. Five deployment booms interface with the flasher. The booms define the translational position of the outer panels of the system. As such, the interfaces between the booms and the flasher do not transmit any torques. A compact spherical joint was designed to act as the interface between the flasher and the booms to prevent any torque transfer (see Figure 2(c)). These joints use 3 ball bearings to allow 3 degrees of rotational freedom during deployment.

Optical interfaces were designed in a modular manner to enable the smooth placement of manufactured optical components within the mechanical framework. First, each optical element is placed within and epoxied to a flexure frame in a clean room. The flexure frame consists of a thin aluminum frame with 3

flexures that couple to the optical element. The flexures provide a means to accommodate manufacturing variability and thermal expansion without damaging optical components. Each flexure frame is then epoxied to an inner frame. Each inner frame is then connected to the outer frame of each panel with another coupling interface. See Figure 2(b) for further details.

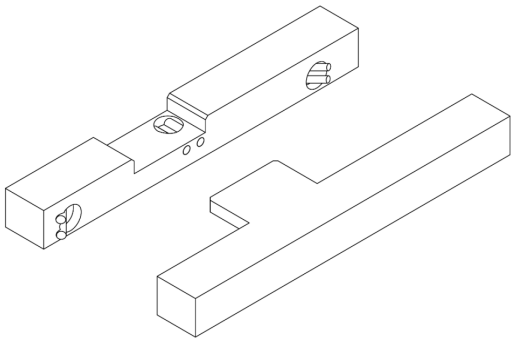

Figure 3. Modified Kinematic Coupling Presented by Roubicek et al. [7]

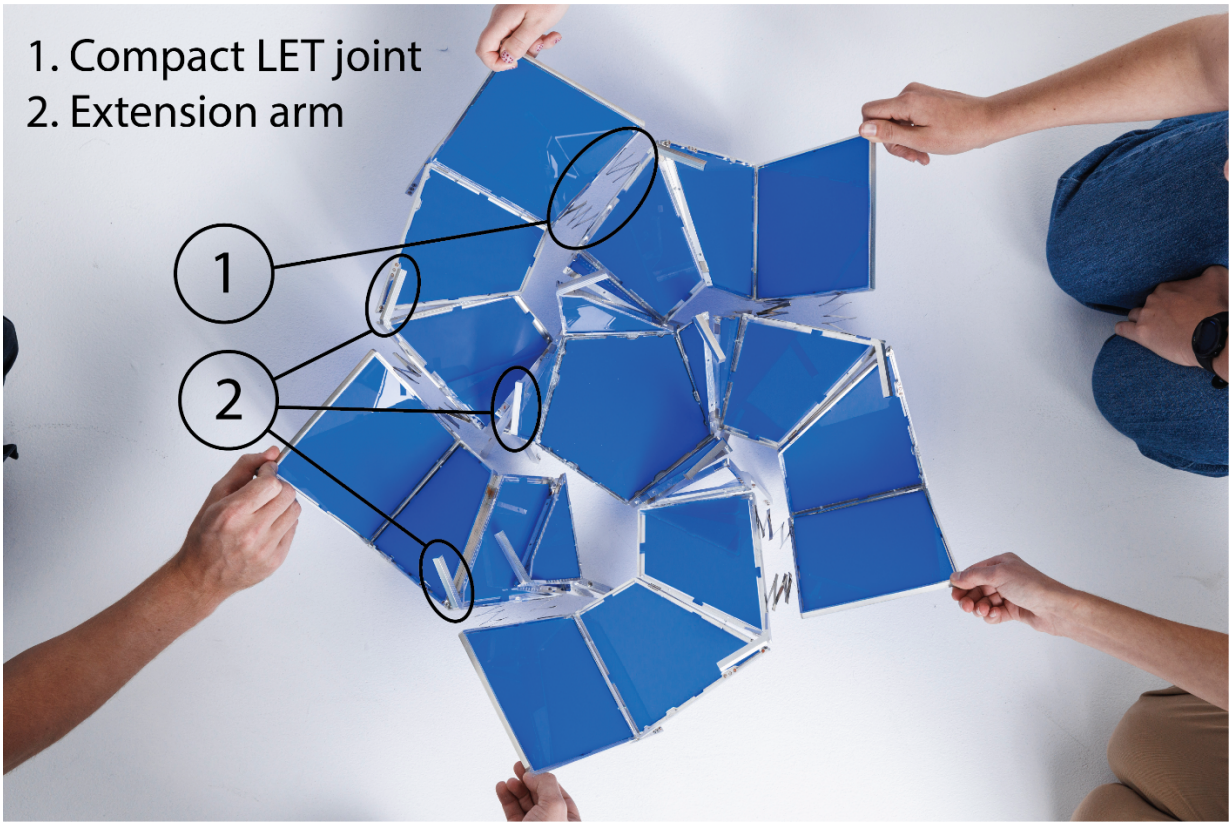

Figure 4. Visual of the Telescope System Partially Deployed, Highlighting Compact LET Joint And Extension Arm Locations

An adjustment system was implemented between each outer aluminum frame and the inner frames just described. Three ball-end set screws are used to enable 3 additional degrees of freedom of adjustment for calibrating optical components prior to launch. Further testing of these components is still underway. See Figure 2(b) for further details.

System Integration

The telescope system was manufactured and assembled in stages, as follows:

1. Rigid aluminum outer frames were machined and deburred.
2. Bushings were glued into outer frames using LOCTITE™ 680. Magnets and stainless steel spheres were glued into corresponding machined cavities using cyanoacrylate. Set screws were threaded into corresponding bushings.
3. Each petal was assembled by tying adjacent panels together with SpiderWire™.
4. Each petal was folded to verify correct engagement of kinematic couplings.
5. Kinematic coupling groove surfaces were work hardened through repeated actuation, as recommended by Slocum [21].
6. Each petal was connected to the central polygon using SpiderWire™. All petals were connected together by compliant hinges adhered with JB Weld™.
7. Inner frames, optical flexure frames, and optical components will be placed within panels at a future date.

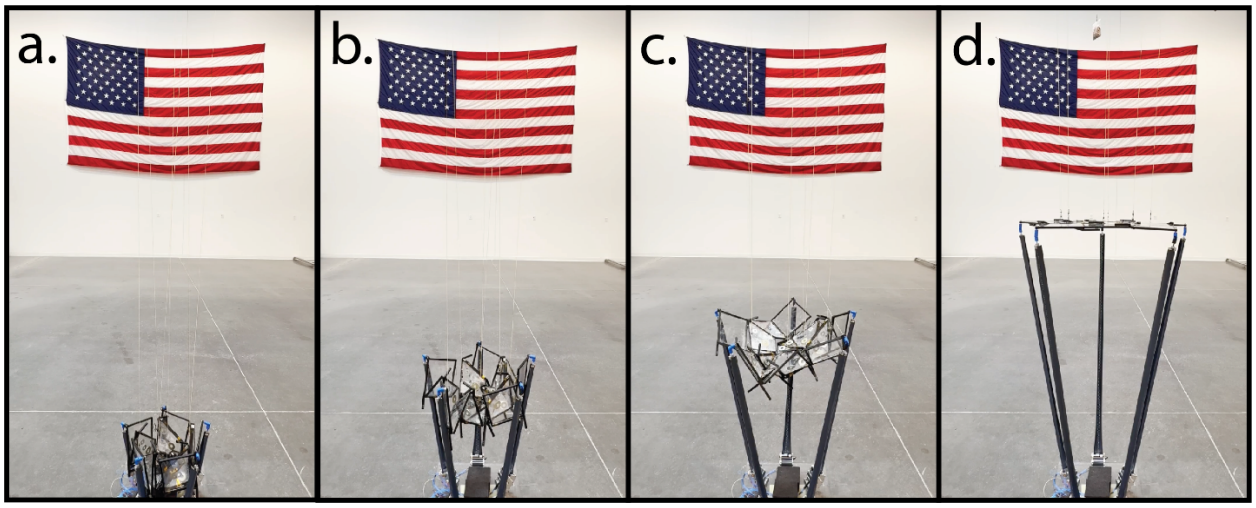

Figure 5. Images of the telescope system throughout a gravity-offset deployment test. (a-d) progress from stowed to deployed states. System diameter in the deployed state is approximately 0.6 m

Testing was then conducted on the system as a whole, and future testing is still anticipated. Both are listed below:

1. The telescope system is deployed on a low friction surface using a pulley system. The purpose of this stage of deployment tests was to visually verify the kinematic motion of each panel during deployment and alignment between panels once deployed.
2. The telescope system is deployed in a gravity offset environment in a horizontal orientation. These are conducted at MMA Space™ and shown in Figure 5. Scans of the system are performed after each deployment to measure panel alignment.

3. The telescope system is deployed in a gravity offset environment in a vertical orientation. Scans of the system are performed after each deployment to measure panel alignment.
4. Once optical components are integrated into the system, optical performance tests will be performed at NASA Goddard Space Flight Center.

Discussion

Several important observations were made throughout the design, analysis, and testing process. First, the crease pattern selected for this work is non-rigid foldable. This means that a zero-thickness model thereof cannot fold without panel deformation. However, by using compliant hinges, we instead used hinge deformation. Second, reducing the size of a traditional kelvin precision coupling can reduce stability across the coupling. However, without the need to support significant loads, a compact coupling was shown to enable sufficient precision. Furthermore, introducing extension arms can improve stability about the least stable axis. Third, conducting deployment tests throughout the design process can help identify areas of weakness that may not be apparent during initial modeling.

Conclusion

Current test results have demonstrated the feasibility to design a functional origami-based deployable optical space system. Rigid aluminum frames replicate origami geometry and house precision elements. Precision couplings are capable of a standard deviation of less than 10 μm displacement along, and 0.005° rotation about, each axis. Compliant hinges ensure appropriate folding and thickness accommodation. Deployment booms interface with and successfully deploy the telescope. Flexure frames appropriately accommodate for manufacturing variability, and set screws enable micro-adjustability for optical elements.

Acknowledgements

This material is based upon work supported by the NASA Earth Science Technology Office under award number 80NSSC23K1235 and a NASA Space Technology Graduate Research Opportunities Award under grant number 80NSSC24K1336.

References

1. J. Kalirai, Scientific discovery with the James Webb space telescope, Contemporary Physics 59 (3) (2018) 251–290. doi:10.1080/00107514.2018.1467648.
2. J. P. Gardner, J. C. Mather, M. Clampin, R. Doyon, M. A. Greenhouse, H. B. Hammel, J. B. Hutchings, P. Jakobsen, S. J. Lilly, K. S. Long, et al., The James Webb space telescope, Space Science Reviews 123 (4) (2006) 485–606.
3. F. Simonetti, A. Z. Marchi, L. Gambicorti, V. Bratina, P. Mazzinghi, Large aperture telescope for advanced lidar system, Optical Engineering 49 (7) (2010) 073001, publisher: SPIE. doi:10.1117/1.3461976.
4. A. Fix, G. Naletto, I. Hutchinson, N. Karafolas, W. Riede, A. Heliere, B. Menzies, H. Riris, Space Lidar and Space Optics, CEAS Space Journal 11 (4) (2019) 359–362. doi:10.1007/s12567-019-00288-2.
5. T. Tomida, Y. Tsuyuguchi, T. Arai, T. Benno, M. Chikawa, K. Doura, M. Fukushima, K. Hiyama, K. Honda, D. Ikeda, et al., The atmospheric transparency measured with a lidar system at the telescope array experiment, Nuclear Instruments and Methods in Physics Research Section A: Accelerators, Spectrometers, Detectors and Associated Equipment 654 (1) (2011) 653–660.
6. G. K. Schwemmer, R. D. Rallison, T. D. Wilkerson, D. V. Guerra, Holographic optical elements as scanning lidar telescopes, Optics and lasers in engineering 44 (9) (2006) 881–902.
7. C. Roubicek, P. B. Klocke, D. Wing, S. P. Magleby, L. L. Howell, Design and testing of a precision coupling for origami-based arrays, Mechanism and Machine Theory 206 (2025) 105936. doi:10.1016/j.mechmachtheory.2025.105936.
8. J. Morgan, S. Magleby, L. Howell, An approach to designing origami-adapted aerospace mechanisms, Journal of Mechanical Design 138 (5) (2016). doi:10.1115/1.4032973.
9. D. Misseroni, P. P. Pratapa, K. Liu, B. Kresling, Y. Chen, C. Daraio, G. H. Paulino, Origami engineering, Nature Reviews Methods Primers 4 (1) (2024) 40.
10. S. Yue, A Review of Origami-Based Deployable Structures in Aerospace Engineering, Journal of Physics: Conference Series 2459 (1) (2023) 012137. doi:10.1088/1742-6596/2459/1/012137.
11. E. B. Crampton, S. P. Magleby, L. L. Howell, Realizing origami mechanisms from metal sheets, in: International Design Engineering Technical Conferences and Computers and Information in Engineering Conference, Vol. 58189, American Society of Mechanical Engineers, 2017, p. V05BT08A055.
12. S. Leanza, S. Wu, X. Sun, H. J. Qi, R. R. Zhao, Active materials for functional origami, Advanced Materials 36 (9) (2024) 2302066.
13. R. J. Lang, K. A. Tolman, E. B. Crampton, S. P. Magleby, L. L. Howell, A review of thickness accommodation techniques in origami-inspired engineering, Applied Mechanics Reviews 70 (1) (2018) 010805.
14. T.-H. Kim, K.-I. Jang, D.-Y. Lee, J.-H. Han, Rigid-Foldable Polyhedral Origami, AIAA Journal 61 (12) (2023) 5645–5657. doi:10.2514/1.J063223.
15. R. J. Lang, S. Magleby, L. Howell, Single degree-of-freedom rigidly foldable cut origami flashers, Journal of Mechanisms and Robotics 8 (3) (2016) 031005.
16. S. A. Zirbel, R. J. Lang, M. W. Thomson, D. A. Sigel, P. E. Walkemeyer, B. P. Trease, S. P. Magleby, L. L. Howell, Accommodating thickness in origami-based deployable arrays, Journal of mechanical design 135 (11) (2013) 111005.
17. H. Pruett, P. Klocke, L. Howell, S. Magleby, Characterization of magnetically stabilized hinges for origami inspired mechanisms, Philosophical Transactions of the Royal Society A: Mathematical, Physical and Engineering Sciences 382 (2283) (2024).
18. J. O. Jacobsen, G. Chen, L. L. Howell, S. P. Magleby, Lamina emergent torsional (let) joint, Mechanism and Machine Theory 44 (11) (2009) 2098–2109.
19. L. Q. Gardner, K. Varela, L. L. Howell, S. P. Magleby, Compact let arrays for origami-based mechanisms, Robotics 15 (1) (2025) 1.
20. T. Ring, E. Ruhl, J. Banik, Structural performance of the nanosat deployable truss, in: 2018 AIAA Spacecraft Structures Conference, 2018, p. 1679.
21. A. H. Slocum, Design of three-groove kinematic couplings, Precision Engineering 14 (2) (1992) 67–76. doi:10.1016/0141-6359(92)90051-W.